Biochimica et Biophysica Acta, 1015 (1990) 205–215
Elsevier

BBABIO 43131

The effect of pH on redox titrations of haem *a* in cyanide-liganded cytochrome-*c* oxidase: experimental and modelling studies

A. John Moody and Peter R. Rich

Glynn Research Institute, Bodmin (U.K.)

(Received 1 July 1989)

Key words: Cytochrome *c* oxidase; Heme *a*; Copper center; Redox potentiometry; Cyanide

Isolated cytochrome-*c* oxidase ligated with cyanide was titrated by Flash-Induced chemical photoREduction (FIRE) (Moody, A.J. and Rich, P.R. (1988) EBEC Short Rep. 5, 69) using cytochrome *c* as a redox indicator. Haem *a* is found to titrate in a complex manner consistent with its interacting anticooperatively with at least two other components. We assign Cu_B as the major interactant at neutral pH, and Cu_A as the minor interactant. In the pH range 7.0–8.1 the strength of the interaction with Cu_B is found to decrease with increasing pH, while the interaction with Cu_A remains essentially constant. The decrease in the interaction with Cu_B appears to continue above pH 8.1 such that at pH 9.2 the titration curve for haem *a* is only slightly distorted from an '*n* = *1*' shape, although it is not possible from the titration data to assess the relative contributions of Cu_B and Cu_A to the total interaction observed at pH values greater than 8.1. Haem *a* and Cu_B show similar pH-dependence and, to account for this, we present a model in which the oxidoreductions of both haem *a* and Cu_B are linked to the (de)protonation of a common acid/base group. The model predicts a pH-dependent indirect cooperative interaction between haem *a* and Cu_B in addition to the direct anticooperative interaction, thereby explaining the observed pH-dependence of the redox interaction between haem *a* and Cu_B.

Introduction

Cytochrome-*c* oxidase (EC 1.9.3.1), the terminal electron acceptor of the mammalian electron transfer chain, contains four redox-active components, two haems, *a* and a_3, and two copper centres, Cu_A and Cu_B ([1], but see Ref. 2 for evidence of a fifth centre). It is well established that there is an electronic interaction between the two haems such that reduction of one makes reduction of the other more difficult. This, the neoclassical model [3], has been used successfully [4] to explain quantitatively why haem *a* titrates in a biphasic manner in unliganded oxidase [5,6], where haem a_3 is redox-active, but almost as a simple Nernstian component ('*n* = *1*') in CO-liganded oxidase [5], where haem a_3 is held in the reduced form.

A prediction of the neoclassical model is that haem *a* should also titrate as an '*n* = *1*' component in cyanide-liganded cytochrome oxidase, where haem a_3 is held in the oxidised form. However, in this state haem *a* is found to titrate in a distorted manner which can be fitted approximately with an '*n* = *0.5*' curve [7–9] (but see exceptions, Refs. 10, 11). This behaviour is seen as resulting from the anticooperative interaction between haem *a* and another centre, which Goodman [12] has shown, from EPR data, to be Cu_B [13–15]. A further extension to the neoclassical model, to include an anticooperative interaction between haem *a* and the other copper centre, Cu_A, has been made by Chan and coworkers [13] to explain slight distortions that they have observed in the titration curves of haem *a* and Cu_A in CO-liganded oxidase [15,17].

We have been conducting a systematic study of the effects of membrane potential ($\Delta\psi$) and transmembrane pH gradient (ΔpH) on the midpoint potentials of the redox centres in cytochrome oxidase. Recently, as part

Abbreviations: $\Delta\psi$ and ΔpH, the difference in electric potential and pH across a membrane, respectively; PES, 5-ethyl phenazinium ethosulphate; TMPD, *N,N,N',N'*-tetramethyl-*p*-phenylenediamine.

Correspondence: A.J. Moody, Glynn Research Institute, Bodmin, Cornwall PL30 4AU, U.K.

of this ongoing research strategy aimed at locating the proton pumping activity of the enzyme [18], we observed a considerable decrease in the distortion of the haem *a* titration curve in cyanide-liganded mitochondria on imposition of a protonmotive force across the inner membrane [19]. Since the distortion in the haem *a* titration curve is due, at least in part, to Cu_B, we began a study of the redox behaviour of Cu_B in cyanide-liganded oxidase, with a view to understanding this phenomenon. Cu_B has no measurable optical signal so we have attempted to study its behaviour by analysis of haem *a* titration curves.

We applied the technique of flash-induced chemical photoreduction [20,21] (FIRE, [22]) to the reductive titration of cyanide-liganded oxidase, using cytochrome *c* as an indicator of redox potential. The results, which we present here, are novel for several reasons.

(a) High quality titration data have been obtained for isolated oxidase over a wide range of pH (6.2–9.2). The quality of the data is the result of: (1) the use of the FIRE technique, which has the advantage, since only light is used to promote reduction, that the titration vessel is not mechanically disturbed after the initial additions; (2) the use of the indicator method, which avoids the problems of mediation often associated with electrode measurements; and (3) the use of essentially simultaneous triple-wavelength measurements of haem *a* and cytochrome *c*, which give exceptionally stable baselines, and which allow deconvolution of these two components.

(b) The behaviour of haem *a* is not entirely explained by a single interaction with another component. Instead, we conclude that interactions between two other components and haem *a* are required to explain the titration curves, the major interaction at neutral pH being with a component of similar potential to haem *a*, probably Cu_B, as previously concluded [12], and the minor interaction being with a component with a pH-independent midpoint potential of about 230 mV, consistent with the known properties of Cu_A [23,24].

(c) The shape of the haem *a* titration curve is found to be pH-dependent. While the curve observed at pH 7.5 or less has an approximately '$n = 0.5$' shape, as previously reported [9], that observed at pH 9.2 is only slightly distorted from simple '$n = 1$' behaviour. This appears to be caused by a decrease in the strength of the interaction between haem *a* and Cu_B as the pH increases from neutrality. To explain this, we present a minimal model in which the oxidoreduction of haem *a* and the oxidoreduction of Cu_B are linked to the (de)protonation of a common acid/base group. We propose that the decrease in the interaction energy at high pH arises from the combination of a direct anticooperative interaction between the centres and an indirect cooperative interaction occurring via the common acid/base group.

Preliminary accounts of this work have already been presented [25,26].

Materials and Methods

Keilin-Hartree particles were prepared from bovine heart as described in [27]. Cytochrome-*c* oxidase was isolated from the particles essentially by the method of Kuboyama et al. [28]. Cyanide-liganded oxidase was prepared by incubation with 45 mM KCN for 3–6 days at pH 7.0–7.5 and 4°C.

Reductive titration of haem a using FIRE

The titrations were carried out in a stirred Thunberg cuvette thermostatted at 20°C. Buffered medium containing 75 μM riboflavin and 1 mM potassium EDTA was placed in the cuvette. For pH ≤ 7.5, 0.1 M potassium phosphate was used as buffer. Potassium glycylglycine/potassium phosphate (0.1 M each) was used for pH ≥ 7.5. PES, cytochrome *c* and potassium ferricyanide were then added (3 nmol, 8 nmol and 10 nmol, respectively; final concentrations 2, 5 and 7 μM, respectively). The level of oxygen in the cuvette was reduced by bubbling with nitrogen for 2 min before sealing. Optical measurements were then begun (see below). The sequence of operations was generally as follows (see, for example, Fig. 1A).

(1) Full reduction of cytochrome *c* in a single step or a few steps by FIRE.

(2) Full re-oxidation of cytochrome *c* by addition of ferricyanide.

(3) Addition of cyanide-liganded cytochrome-*c* oxidase (final concentrations of oxidase and cyanide about 2.3 μM and 1.2 mM, respectively).

(4) Full reduction of cytochrome oxidase and cytochrome *c* in small steps by FIRE.

(5) Partial re-oxidation of cytochrome oxidase and cytochrome *c* by oxygen.

(6) Full re-oxidation of cytochrome oxidase and cytochrome *c* in a single step by addition of ferricyanide.

Comments on the method

The FIRE system, riboflavin/EDTA, is based on that of Ahmad et al. [20,21]. PES was added to improve the end-point of the titration [22]. At pH 6.2 there is significant overlap between the PES and haem *a* titration curves, so pyocyanine, which has a lower midpoint potential [29], was used instead. Additions subsequent to the initial sealing of the cuvette were made through a nitrogen atmosphere. However, the additions themselves were aerobic because low-oxygen rather than anoxic conditions were wanted. This minimises autoxidation of FIRE intermediates while keeping haem a_3-cyanide clamped in the oxidised state. Cytochrome *c* was used as a redox indicator/mediator. The main problem with this is that cyanide slowly ligates ferricy-

tochrome *c*. However, a correction for this can be made as described in Appendix 1.

Optical measurements

Optical measurements were made with a single-beam spectrophotometer constructed round a Bentham M300HR monochromator (Bentham Instruments, Reading, U.K.) fitted with a G312R0u75 ruled grating (1200 lines/mm; blazed at 750 nm). The detector was a photodiode with integral amplifier (E.G.&G. Photon Devices HUV-4000B; supplied by Metax, Tunbridge Wells, U.K.). Cytochrome *c* and haem *a* were monitored by using a cycle of eleven measurements at 540, 550, 558, 582, 606, 630, 606, 582, 558, 550 and 540 nm. The triple-wavelength absorbance [19] for each component, ΔA_T, was then calculated from these signals using the formula:

$$\Delta A_T = A_C - A_L + (A_H - A_L)\cdot(\lambda_C - \lambda_L/\lambda_H - \lambda_L) \quad (1)$$

where A_L, A_C and A_H are the average absorbances at λ_L, λ_C and λ_H, respectively. For cytochrome *c*, λ_L, λ_C and λ_H are 540, 550 and 558 nm, respectively. For haem *a* they are 582, 606 and 630 nm, respectively. The triple-wavelength technique was used because it effectively eliminates baseline drift due to changes in light scattering. Note that the time taken for a set of three measurements (5 s at most) is short compared to the rate of change of absorbance. In addition, the possibility of systematic error is reduced further by taking the average of the two measurements at the same wavelength in a given cycle.

After every fifth cycle of measurements sampling was stopped temporarily to allow additions to be made or the cuvette to be flashed.

Flash system

The flash system consisted of an E.G.&G. Xenon guided-arc lamp FX-200 and Lite-Pac FY-604; an E.G.&G. Electro-optics PS-350 power supply (operated at 1000 V) and triggering circuitry, powered by a Coutant GPE 500/24 power supply (supplied by STC Instrument Services, Harlow, U.K.); and a 15 μF working capacitor (LASER discharge type) (supplied by Hivolt Capacitors, Londonderry, N. Ireland). The white flashes were filtered with a 520 nm short pass filter and directed perpendicular to the measuring beam using a glass-fibre light guide. The detector was protected from the flash using a GG495 or GG475 Schott glass high-pass filter.

Spectral deconvolution

The wavelengths used were selected by examination of the pure reduced-oxidised spectra of cytochrome *c* and haem *a*. The spectrum of haem *a* was generated by FIRE of cyanide-liganded oxidase in the absence of cytochrome *c* (Fig. 4). The contribution by {cyt c^{2+} – cyt c^{3+}} to the haem *a* wavelength triplet ($\varepsilon_{T,\text{haem } a} \simeq \varepsilon_{606\text{-}630} \simeq 20\ \text{mM}^{-1}\cdot\text{cm}^{-1}$ [30]) is small but significant ($\varepsilon = 0.54\ \text{mM}^{-1}\cdot\text{cm}^{-1}$), whereas the contribution of {haem a^{2+} – haem a^{3+}} to the cytochrome *c* wavelength triplet ($\varepsilon_{T,\text{cyt } c} = 20.2\ \text{mM}^{-1}\cdot\text{cm}^{-1}$ [31]) is negligible ($\varepsilon = -0.01\ \text{mM}^{-1}\cdot\text{cm}^{-1}$). It is therefore a simple matter to correct the haem *a* measurements for the contribution by cytochrome *c*.

Results and Discussion

Comments on the validity of the titration data

The effects of pH on the aerobic reductive titration of haem *a* in cyanide-liganded cytochrome-*c* oxidase were studied. Cytochrome *c* was used as a redox indicator/mediator. The problem with this is that cyanide slowly ligates ferricytochrome *c*, the product of the reaction being essentially redox inactive in the range of potentials met during these experiments. However, it is possible to allow for this and the correction procedure used is described in the Appendix 1. It should be noted that at low pH (≤ 7.5) less than 10% of the cytochrome *c* was converted to cyanoferricytochrome *c* by the end of the titrations so that the correction was almost negligible. At high pH (9.2, i.e., close to the optimum for the reaction of cyanide with cytochrome *c* [32]) about 50% of the cytochrome *c* was converted to cyanoferricytochrome *c*, so that the correction was somewhat larger (Fig. 2B, compare open and closed symbols). The correction procedure has been validated at pH 7.5 by titrating cytochrome *c* in the presence of cyanide, using TMPD as redox indicator, in which case, after correction, good quality '$n = 1$' curves were obtained. Note that TMPD is unstable at potentials above about 400 mV [33], the instability increasing as pH increases, making it unsuitable as a redox indicator for the redox titration of cyanide-liganded cytochrome-*c* oxidase.

At low pH (≤ 7.5) a significant level of autoxidation was observed, despite the presence of cyanide (Fig. 1A). Here, it proved possible to let the system back-titrate to around 50% haem a^{2+} before the rate of autoxidation became negligible *, and, in such cases, there was negligible hysteresis in the titration curves (Figs. 1B '1' and 2A, compare open and closed symbols in the latter). Above pH 7.5 the extent to which back-titration using autoxidation was possible decreased such that it was insignificant at pH 9.2. Where autoxidation was negligible, successive data at a given potential showed no time-dependence (Fig. 1B '2'). This, and the lack of

* Presumably, the rate of autoxidation relates to occupancy of the haem a_3^{2+}-cyanide state, in which haem a_3 has a low affinity for cyanide [48].

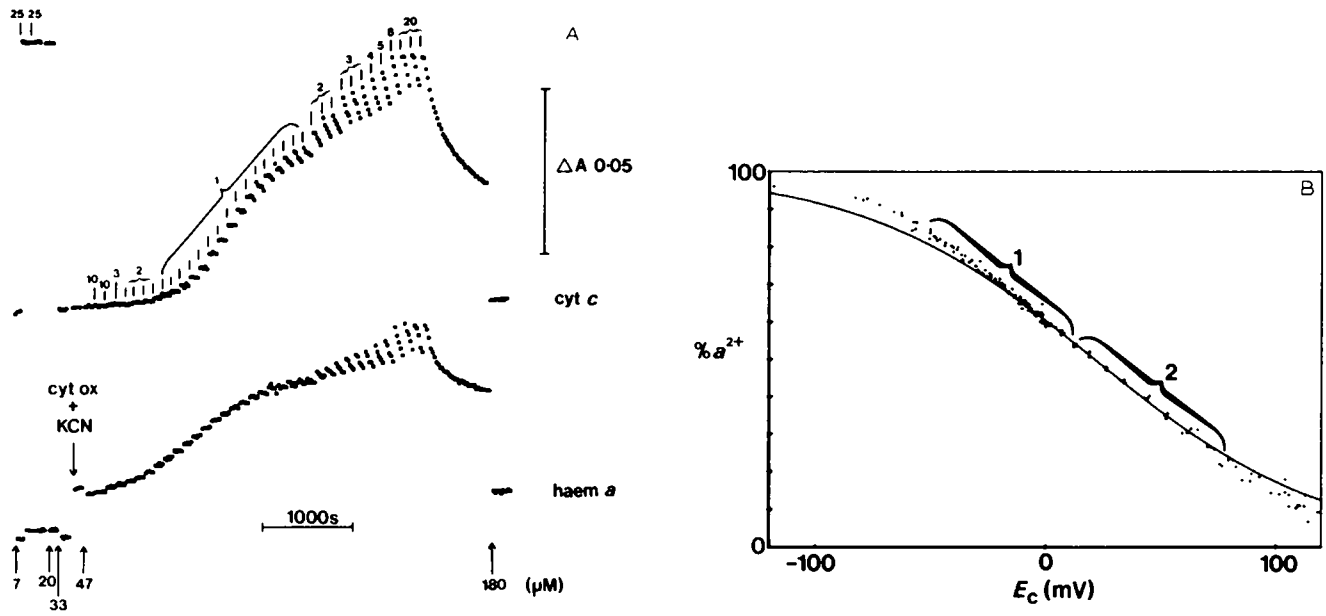

Fig. 1. (A) Raw data from a titration of haem *a* (2.3 μM) in cyanide-liganded cytochrome-*c* oxidase at pH 7.5 and 20 °C in 0.1 M potassium glycylglycine containing 0.1 M potassium phosphate, 1 mM potassium EDTA. 1 mM KCN, 5 μM cytochrome *c*, 2 μM PES, and 75 μM riboflavin. The triple-wavelength signals (ΔA_T) for cytochrome *c* and haem *a* are shown. These were derived from measurements at 540, 550 and 558 nm, and 582, 606 and 630 nm, respectively (see Materials and Methods). The 'ticks' on the upper trace mark when the sample was photoreduced; the numbers indicate the quantity of flashes used. Cyanide-liganded oxidase was added as indicated. The arrows on the lower trace mark additions of potassium ferricyanide; the cumulative final concentrations in the sample are shown. The titration curve derived from these data, after deconvolution and correction for ligation of cytochrome *c* by cyanide, is shown in (B) (see also Fig. 2, ▲). E_c is defined as the potential relative to cytochrome *c*, i.e., $58 \cdot \log_{10}(\text{cyt } c^{3+}/\text{cyt } c^{2+})$ at 20 °C. The solid line is an '*n* = *0.5*' curve with midpoint 22 mV more positive than the midpoint of cytochrome *c*. The regions labelled '1' and '2' are referred to in the text.

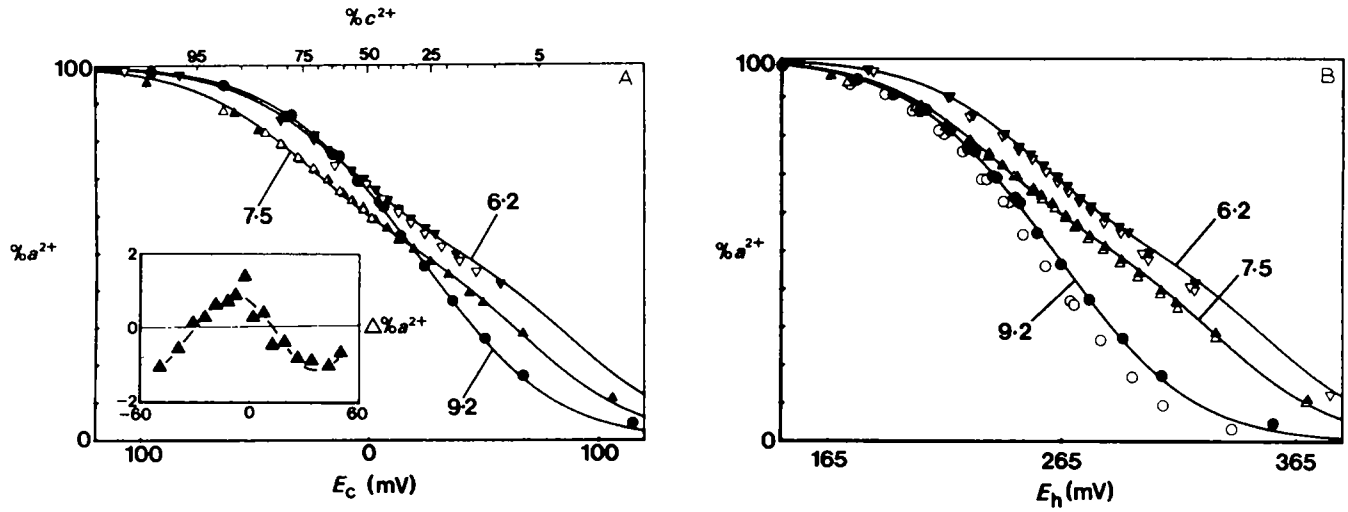

Fig. 2. Plots of percentage haem *a* reduction versus E_c (A) and E_h (B) for titrations at pH 6.2, ▼; pH 7.5, ▲; and pH 9.2, ●. E_c is as defined in Fig. 1B. The data within each successive 5% range of percentage cyt *c* reduction, starting at 0–5%, were averaged. This tends to give more weight to data at potentials close to the E_m of cytochrome *c*, since there are usually more data at the extremes. The solid lines in each case were obtained by fitting to the averaged reductive data on the basis that haem *a* interacts anticooperatively with another, unseen, component. See Appendix 2 for method of simulation. $E_{m,0}$ and $E_{m,R}$ are the midpoint potentials for one component with the other oxidised and reduced, respectively. The fit parameter values relative to $E_{m,cyt\,c}$ at the pH given were: pH 6.2 haem *a*, $E_{m,0}$ = 73 mV and $E_{m,R}$ = 5 mV, and interactant, $E_{m,0}$ = 72 mV; pH 7.5 haem *a*, $E_{m,0}$ = 53 mV and $E_{m,R}$ = −12 mV, and interactant, $E_{m,0}$ = 51 mV; and pH 9.2 haem *a*, $E_{m,0}$ = 28 mV and $E_{m,R}$ = 9 mV, and interactant, $E_{m,0}$ = 17 mV, E_h was calculated using $E_{m,7}$ = 265 mV for cytochrome *c* and $pK_{app.}$ for ferricytochrome *c* = 9 (Ref. 46 and own measurements on 695 nm band). Note that $E_{m,6.2}$ and $E_{m,7.5}$ for cytochrome *c* are about 24 mV higher than $E_{m,9.2}$. The open and filled symbols in (A) are averaged oxidative and reductive data, respectively; in (B) they are averaged reductive data, uncorrected and corrected for ligation of cytochrome *c* by cyanide, respectively. The inset in (A) shows the residuals for the pH 7.5 data.

hysteresis, indicate that the system was in rapid equilibrium.

A qualitative description of the titration curves

Sample titration curves are shown in Figs. 1B, 2 and 6. The effects of pH in the range 6.2–9.2 can be divided into two phases. Between pH 6.2 and 7.5 the titration curve has the approximate '$n = 0.5$' form previously described [9]. The observed midpoint potential decreases by 15–20 mV in this range. As the pH is increased above 7.5 the titration curve becomes more like a simple '$n = 1$' curve. Again, the observed midpoint potential shows slight negative pH-dependence, decreasing by about 25 mV in the pH range 7.5–9.2. Overall, the average pH-dependence of the observed midpoint at about −13 mV/pH unit (Fig. 3) is lower than the −30 mV/pH unit value reported by Artzatbanov et al. [9] for cyanide-liganded oxidase in situ in mitochondria.

The pH-dependent change in the shape of the haem *a* titration curve was not observed by Artzatbanov et al., using conventional redox potentiometry with a Pt electrode. However, the limited results (two pH values) of Wikström [15], also for mitochondria but using endogenous cytochromes *c* and c_1 as redox indicators, confirm the results presented here. In addition, conventional redox titrations carried out in our laboratory on isolated oxidase and on mitochondria also show the same shape change (Mitchell, R., unpublished results).

Quantitative interpretation of the titration curves in terms of interacting redox centres

To a first approximation, at each pH studied, the data presented here can be interpreted in two ways:

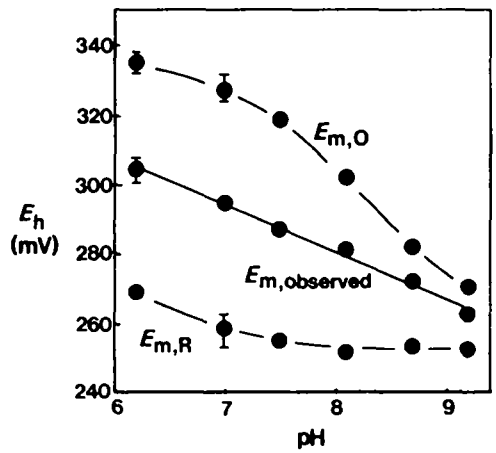

Fig. 3. The effect of pH on $E_{m,observed}$, $E_{m,0}$ and $E_{m,R}$ for the titration of haem *a* in cyanide-liganded oxidase. $E_{m,0}$ and $E_{m,R}$ were obtained from fits to the titration curves on the basis that haem *a* interacts anticooperatively with another component (see text and Fig. 2 legend). $E_{m,observed}$ is self-explanatory: the solid line was obtained by linear regression and has a slope of −13.4 mV/pH unit. The bars represent the range of values obtained for 3, 4, 4, 3, 3 and 2 titrations at pH 6.2, 7.0, 7.5, 8.1, 8.7 and 9.2, respectively.

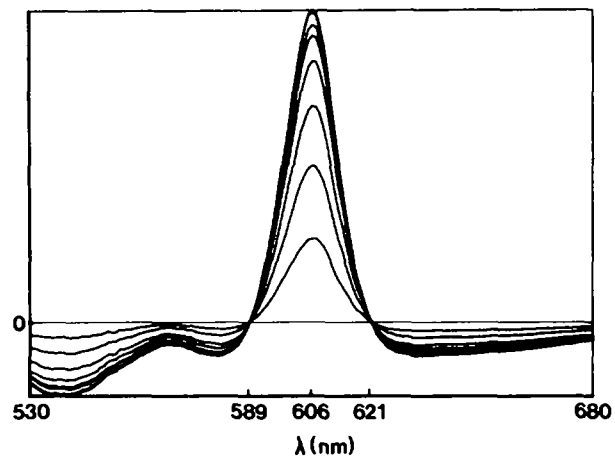

Fig. 4. Redox spectra of haem *a* generated by FIRE of cyanide-liganded cytochrome oxidase in the absence of cytochrome *c*. The medium was as described in the legend to Fig. 1. The concentrations of oxidase and KCN were 6 μM and 6 mM, respectively. The sample was flashed eight times between each spectrum.

either as the reduction of 2 one-electron ('$n = 1$') components or as the reduction of a single '$n = 1$' component interacting anticooperatively with another unseen '$n = 1$' component (interactant). The latter interpretation is appropriate because haem a_3 is held oxidised by the bound cyanide, and so we expect to observe only haem *a*. This is largely confirmed by the spectra obtained in the range 530–680 nm on flash-reduction of cyanide-liganded oxidase in the absence of cytochrome *c* (Fig. 4). However, it should be noted that there is a slight blue shift (< 1 nm) in the '606 nm' peak as the extent of reduction is increased, which is probably caused by slight spectral interaction, as well as electronic interaction, between haem *a* and the interactant. With respect to our triple-wavelength measurement of haem *a* this peak shift is negligible, but it is also possible that the amplitude of the '606 nm' peak is affected by oxidoreduction of the interactant. We have assumed that this is not the case, the assumption being partly justified by the known insensitivity of the redox spectrum of haem *a* in this region to the redox state of haem a_3 [34]. The solid lines in Fig. 2 are the results of least-squares fits made to the averaged reductive data. A summary of such fits is shown in Fig. 3.

On subtraction of the single-interactant fits from the data it was noted that the residuals obtained at pH 7.0 and 7.5 were consistently non-random (Fig. 2A, inset), and to a lesser extent this was true at pHs 6.2 and 8.1. The residuals at high pH values (8.7 and 9.2) appeared to be random, although the level of noise was higher. The non-random residuals may be explained by the presence of a second, minor, interactant.

Identity of the interactants

The cytochrome oxidase preparation used in these experiments was predominantly in the 'slow' form ('re-

sting' oxidase) as opposed to the 'permanently-fast' form recently described [35,36], which, like 'pulsed' oxidase, binds cyanide rapidly and shows rapid reduction of haem a_3 by dithionite. Because the rate of intramolecular electron transfer from haem a/Cu_A to haem a_3/Cu_B is found to be much too slow in the 'slow' form to be consistent with the observed rate of turnover of the enzyme, this form is not considered to be involved in the normal catalytic cycle. However, it is important to note that the barrier to intramolecular electron transfer is broken, i.e., Cu_B can be titrated, on ligation of oxidase with cyanide [37–39]. There are, therefore, three potential interactants with haem *a* in cyanide-liganded oxidase, namely, haem *a* itself, Cu_A, and Cu_B. A mutual interaction between the two haems *a* in oxidase dimers was proposed by Wikström et al. [1] as a possible explanation for the haem *a* titration curve in the cyanide-liganded enzyme. However, the EPR data of Goodman [12] provide strong support for the assignment of Cu_B as the major interactant at neutral pH, since it was found on titration of cyanide-liganded oxidase that changes in the '$g = 3.0$' signal, i.e., from haem a^{3+}, were mirrored by changes in the '$g = 3.6$' signal, which is thought to indirectly indicate the redox state of Cu_B (i.e., it comes from haem a_3^{3+}-cyanide when the magnetic coupling between haem a_3 and Cu_B is broken by reduction of Cu_B [38,39]).

We favour assignment of Cu_A as the second interactant at neutral pH, since evidence has also been presented for an anticooperative interaction (20–40 mV) between Cu_A and haem *a* in CO-liganded oxidase [16,17], and, as we shall see below, the fitted midpoint potential of the second interactant is in good agreement with published values for Cu_A [23].

A scheme of interactions in cyanide-liganded oxidase

On the basis of spectroelectrochemical titrations of unliganded and, CO-liganded, and unpublished titrations of cyanide-liganded oxidase, Blair et al. [13] have proposed a scheme of anticooperative interactions between the redox components in unliganded cytochrome oxidase in which (a) haem *a*, haem a_3 and Cu_B mutually interact, and (b) haem *a* and Cu_A mutually interact. In cyanide-liganded oxidase, where haem a_3 is held in the oxidised state, we are left with anticooperative interactions between haem *a* and Cu_B, and haem *a* and Cu_A. The similarity in the midpoint potential of Cu_A observed for unliganded and cyanide-liganded oxidase, where Cu_B is redox active, and CO-liganded oxidase, where Cu_B is held reduced, implies that there is no significant interaction between Cu_B and Cu_A [40]. When curves are fitted to the titration data on this basis much better fits than the single-interactant fits are obtained, so our data are at least in qualitative agreement with such a scheme.

It should be noted that there is no unique 'best fit' (minimum in squared residuals) for each set of data, particularly at pH values where the single-interactant fits are satisfactory anyway. However, at pH 7.0, 7.5 and 8.1 two 'best fits' are obtained for all of the sets of data. Of these two fits, one can be eliminated because it predicts a cooperative interaction between Cu_A and haem *a*, whereas anticooperativity was observed by Ellis et al. [16] in the CO-liganded enzyme. The other fit is in good agreement with the interaction scheme proposed by Blair et al. [13]. Further, the predicted midpoint potentials of Cu_B and Cu_A (320 mV and 230 mV, respectively, at pH 7.5) are in excellent agreement with published values for these centres [23,41]. The fitted

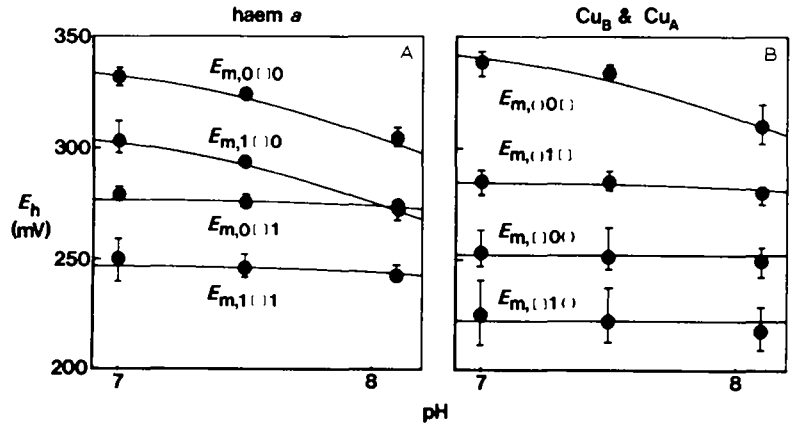

Fig. 5. The effect of pH on fits to the titration of haem *a* in cyanide-liganded oxidase obtained on the basis that haem *a* interacts anticooperatively with two other components (see text). (a) Haem *a* midpoints, and (b) Cu_B and Cu_A midpoints. The nomenclature for the midpoints is as follows. The order of components in the suffix is Cu_A, then haem *a*, and then Cu_B. 0 indicates that the component is oxidised; 1 indicates that the component is reduced; [] indicates that the midpoint refers to oxidoreduction of this component; and () indicates that the redox state of this component is unimportant. For example, $E_{m,[]0()}$ is the midpoint for Cu_A when haem *a* is oxidised, which is independent of whether Cu_B is oxidised or reduced. The bars represent the range of values obtained for 4, 4 and 3 titrations at pH 7.0, 7.5 and 8.1, respectively. The solid lines are the results of simulations using the model shown in Fig. 7 (and using the parameter values given in the legend to that figure).

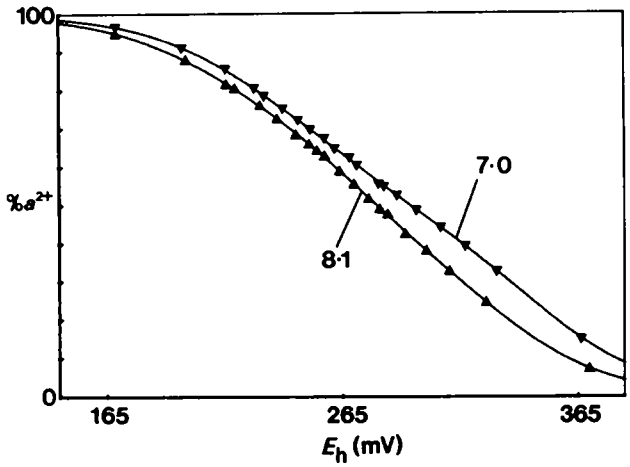

Fig. 6. Plots of percentage haem *a* reduction versus E_h for titrations at pH 7.0, ▼, and pH 8.1, ▲. E_h was calculated as in Fig. 2. Averaged reductive data are shown. The solid lines in each case were obtained by fitting to the averaged data on the basis that haem *a* interacts anticooperatively with two other components (see text). The fit parameter values were: pH 7.0, $E_{m,0[]0} = 328$ mV, $E_{m,0[]1} = 276$ mV, $E_{m,1[]0} = 304$ mV, $E_{m,()0[]} = 332$ mV and $E_{m,[]0()} = 250$ mV; and pH 8.1, $E_{m,0[]0} = 309$ mV, $E_{m,0[]1} = 273$ mV, $E_{m,1[]0} = 276$ mV, $E_{m,()0[]} = 320$ mV and $E_{m,[]0()} = 242$ mV. See Fig. 5 legend for an explanation of this nomenclature. Note that in both cases equally good fits can be obtained using the approximately same values of $E_{m,0[]0}$, $E_{m,()0[]}$ and $E_{m,[]0()}$ but with the interaction between haem *a* and Cu_A, though of the same magnitude, being cooperative, instead of anticooperative. In this case the magnitude of the anticooperative interaction between haem *a* and Cu_B is correspondingly increased so that the same overall interaction is maintained.

parameters for each set of data are summarised in Fig. 5. Fig. 6 shows the averaged data from titrations at pH 7.0 and 8.1 with the two interactant fits overlaid for comparison.

The effects of pH on the potentials of and interactions between the redox centres in cyanide-liganded oxidase: a minimal model

We can see from Fig. 5 that the potential of Cu_A is essentially pH-independent over the pH range 7.0–8.1, in agreement with direct observations by visible and EPR spectroscopy [23,24]. In addition, the strength of the interaction between Cu_A and haem *a* is also pH-independent in this range. By contrast, the midpoint potentials of haem *a* when Cu_B is oxidised ($E_{m,0[]0}$ and $E_{m,1[]0}$) behave as if there were an acid/base group on the enzyme with a p*K* of about 7.5 when haem *a* is oxidised. The midpoint potential of Cu_B when haem *a* is oxidised ($E_{m,()0[]}$) shows a similar pH-dependence. Also the strength of the interaction between haem *a* and Cu_B decreases markedly as pH increases. These trends appear to continue above pH 8.1, although it is impossible from the haem *a* titration data alone to assess the relative contributions of Cu_A and Cu_B to the interaction observed at haem *a*.

Fig. 7 shows a minimal model to explain the effect of pH in the range 7.0–9.2 on the midpoint potentials of haem *a* and Cu_B (for simulations see the solid lines in Fig. 5). In this model the oxidoreduction of haem *a* and the oxidoreduction of Cu_B are linked to the (de)protonation of a common acid/base group. In other words, the model system can exist in two states that are interconverted by (de)protonation of a single acid/base group, the two states being characterised by differing redox midpoint potentials for the redox couples. The titration data are diagnostic of this type of model because the pH-dependence of the oxidoreduction of haem *a* is obviously very different when Cu_B is oxidised compared to when Cu_B is reduced. If haem *a* and Cu_B were linked to entirely different acid/base groups, we would expect the pH-dependence of haem *a* to be independent of the redox state of Cu_B. However, the model is minimal in the sense that a model with multiple common acid/base groups could also fit the data.

An interesting feature of the model is that interaction between the redox centres can occur via the linkage of their oxidoreduction to the common acid/base group. More generally, such 'indirect' interaction can occur whenever two redox centres are linked to a common 'event', e.g., ligand binding. Wikström et al. [1] and Wikström [42] considered the possibility of anticooperative interaction by this means when they discussed a similar model to explain the effect of pH on the midpoint potentials of haem *a* and haem a_3 in unliganded

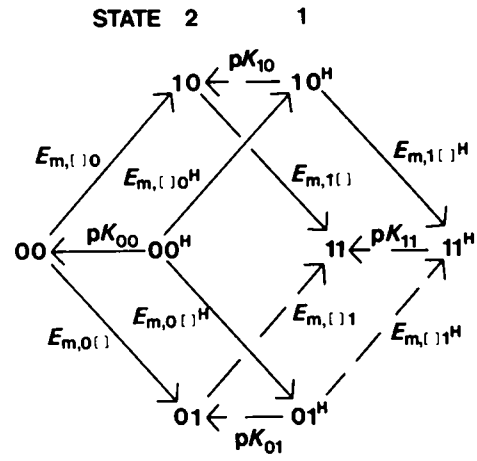

Fig. 7. A two-state model to explain the effect of pH ≥ 7.0 on the titration curve of haem *a* in cyanide-liganded oxidase (see text for details). For clarity Cu_A is omitted. Otherwise, the nomenclature is the same as in Figs. 5 and 6, the order of components being haem *a* and then Cu_B. In state 1 the acid/base group is protonated; in state 2 it is deprotonated. The arrows point in the direction of electronation or deprotonation, as appropriate (see Appendix 2). The parameter values used in the simulations (not best fits) in Fig. 5 were: State 1, $E_{m,0[]0^H} = 339$ mV, $E_{m,1[]0^H} = 309$ mV, $E_{m,0[]1^H} = 277$ mV, $E_{m,1[]1^H} = 247$ mV and $E_{m,()0[]^H} = 347$ mV; State 2, $E_{m,0[]0} = 255$ mV, $E_{m,1[]0} = 225$ mV, $E_{m,0[]1} = 193$ mV, $E_{m,1[]1} = 163$ mV and $E_{m,()0[]} = 265$ mV; and $pK_{00} = 7.55$.

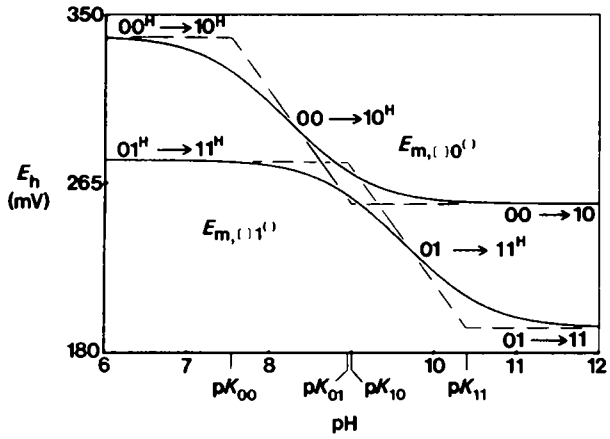

Fig. 8. Simulated E_m/pH profiles for the model given in Fig. 7 (using the parameters given in the legend to that figure). The profiles shown are for haem *a*; for the couple where Cu_A and Cu_B are both oxidised ($E_{m,[]0^0}$), and the couple where Cu_A is oxidised by Cu_B is reduced ($E_{m,[]1^0}$). Note that Cu_A is omitted for clarity, as in Fig. 7. The strength of the interaction is given by the difference between these two midpoints. The strength of the direct interaction between haem *a* and Cu_B is set at −62 mV for either pure state. At pH 9 the apparent interaction reaches a minimum of about −12 mV because of additional indirect cooperative interaction. The dashed lines are idealised E_m/pH profiles (Pourbaix diagrams) for the same couples.

oxidase, but there is no reason, in principle, why the interaction should not be cooperative. In fact, the titration of the Cu_B/haem a_3 binuclear centre in CO-liganded oxidase as an '$n = 2$' component at saturating concentrations of CO [41] is an example of such behaviour.

Cooperative indirect interaction will occur when the common event favours the same redox state of each interactant. This is the case for haem *a* and Cu_B in the cyanide-liganded system – both centres show negative pH-dependence, i.e., protonation of the group favours reduction of the centre and vice versa, and deprotonation of the group favours oxidation of the centre and vice versa. Therefore, we can explain most or all of the decrease in the anticooperative interaction between haem *a* and Cu_B at high pH by the addition of a cooperative indirect interaction in this pH range. To illustrate this, Fig. 8 shows E_m/pH profiles for the parameter values given in the legend to Fig. 7. The direct interaction in both states is set at −62 mV, but this value is observed only when the system is in a single state, i.e., State 1 at pH 6, and State 2 at pH 12.

Note that we have quantitative information on the potentials of haem *a* and Cu_B only in the pH range 7.0–8.1, and semi-quantitative information only up to pH 9.2. Because the model predicts pK values that are at the limit of or outside this range, the range of possible parameter values that give reasonable fits to the data is extremely large. The values chosen here for the simulations in Figs. 5 and 8 are in no way 'best fit' values and hence, the simulation outside the range of observation (e.g., Fig. 8, > pH 9.2) should be regarded as very qualitative predictions.

Although our minimal model can explain the effects of pH in the range 7.0–9.2, it fails to explain the pH-dependence observed between pH 7.0 and 6.2. The minimal model predicts that the midpoint potential of haem *a* when Cu_B is reduced (labelled $E_{m,[]1^0}$ in Fig. 8) should be pH-independent in this range. However, it is clear from Figs. 2B and 6 that the titration curves for haem *a* at pH 6.2, 7.0 and 7.5 are essentially parallel, instead of being coincident at low potential (i.e., where Cu_B is more likely to be reduced) as would be expected. This can also be seen from the fits made to the data on the basis of a single interactant (Fig. 3), where $E_{m,R}$ is pH-dependent in the range 6.2–7.5. It appears, therefore, that at least two acid/base groups are needed to explain the pH-dependence of the haem *a* titration curve in the presence of cyanide over the entire range of pH, 6.2–9.2. This is reminiscent of the two-acid/base-group model used by Wikström et al. [1] to explain the effect of pH on the midpoint potentials of haem *a* and haem a_3 in unliganded oxidase over a similar range of pH.

A summary scheme of the proposed redox interactions in cyanide-liganded oxidase is shown below.

Relationship to proton-pumping activity

The common acid/base group model allows us to make testable predictions as to the quantity of protons taken up at a given pH on reduction of haem *a* or Cu_B alone, or on reduction of both centres together. It is apparent from this model that at physiological pH the acid/base group will be partially protonated when both haem *a* and Cu_B are oxidised but will always be fully protonated when both centres are reduced. It has been speculated (see review by Krab and Wikström [43]) that this represents the 'priming' of a group that is involved

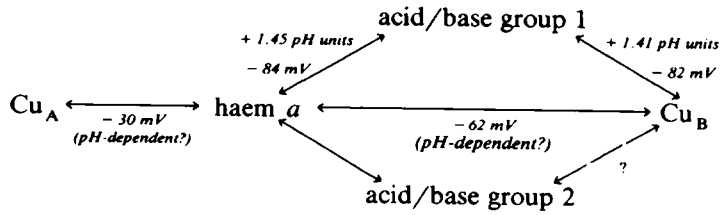

in the proton-pumping function of the oxidase, in which case, the group would presumably have to be located on the matrix side of the enzyme. Indeed, Artzatbanov et al. [9] have presented evidence that the oxidoreduction of haem *a* in situ in mitochondria is sensitive specifically to the matrix pH. However, similar experiments performed in this laboratory [44] indicate the converse, i.e., that haem *a* is only in rapid protonic contact with the extramitochodrial aqueous phase. Also, it is clear, even if the pump were primed in this way, that the major energetic step of the pump cycle must be associated with the reoxidation of Cu_B via the oxygen reducing 'pole' of the oxidase [45,46].

Appendices

(1) Correction for cyanide ligation of cytochrome c

The ligation of ferricytochrome *c* by cyanide has two effects on the titration data. The major effect is to decrease the concentration of cytochrome *c*, since cyanoferricytochrome *c* is essentially redox-inactive in the range of potential encountered in these experiments. There is also a minor contribution by cyanoferricytochrome *c* at both wavelength triplets.

The ligation of ferricytochrome *c* by cyanide is represented by the following kinetic scheme:

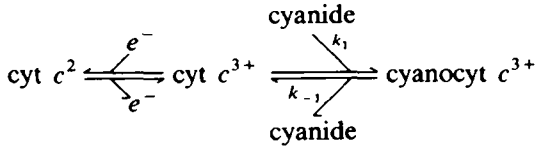

Under the conditions used here the concentration of cyanide is greatly in excess of that of cytochrome *c*, so that k_1 can be replaced with a pseudo-first-order rate constant, k_1', which is equal to $k_1 \cdot$ [cyanide]. The concentrations of unliganded cytochrome *c* or of cyanoferricytochrome *c* after a given time interval, Δt, are given by:

$$[\text{cyt } c]_{t+\Delta t} = [\text{cyt } c]_t \times \exp\{-k_1' \cdot (1/R_2 + R_1/(1+R_1)) \cdot \Delta t\} + \frac{(1+R_1)}{(1+R_1+R_1 \cdot R_2)} \times [\text{cyt } c]_T \times (1 - \exp\{-k_1' \cdot (1/R_2 + R_1/(1+R_1)) \cdot \Delta t\}) \quad (2)$$

$$[\text{cyanocyt } c]_{t+\Delta t} = [\text{cyt } c]_T - [\text{unliganded cyt } c]_{t+\Delta t} \quad (3)$$

where R_1 is the ratio cyt c^{3+} : cyt c^{2+}, R_2 is the equilibrium ratio cyanocyt c^{3+} : cyt c^{3+}, [unliganded-cyt c]$_t$ is the concentration at the beginning of the time interval, and [cyt c]$_T$ is the total concentration of cytochrome *c*, liganded or unliganded. The time-courses of the decrease in unliganded cytochrome *c* and of the formation of cyanoferricytochrome *c* were estimated by calculating the change in concentration in the small time intervals between one datum and the next using Eqns. (2) and (3) (with the approximation that R_1 stays constant during these intervals). The value of k_1' used for a particular set of data was obtained by iteration until there was agreement between (a) the estimated concentration of unliganded cytochrome *c*, i.e., that predicted on the basis of the chosen k_1' and the initial concentration, the latter being measured by fully reducing the cytochrome *c* before the addition of the cyanide-liganded oxidase; and (b) the final concentration of unliganded cytochrome *c*, i.e., that observed when the cytochrome *c* was fully reduced at the end of the titration.

When R_2 is large, Eqn. 2 reduces to Eqn. 4

$$[\text{cyt } c]_{t+\Delta t} = [\text{cyt } c]_t \times \exp\{-k_1' \cdot (R_1/(1+R_1)) \cdot \Delta t\} \quad (4)$$

At pH $\geq$ 7.5 this condition is approximately satisfied, i.e., R_2 is greater than 10 (Ref. 32, pH 7.5; own observations at pH > 8). Values of R_2 at pH 6.2 and 7.0, approx. 1 and 5, respectively, were estimated from K_{KCN} data reported by George and Tsou [32].

The {cyanoferricyt *c* − ferricyt *c*} difference spectrum is pH-dependent; ferricytochrome *c* undergoes a pH-dependent isomerisation. The contributions by cyanoferricytochrome *c* at the cytochrome *c* and haem *a* wavelength triplets were estimated from difference spectra at pH 8.7 and pH 10 on the assumption that the $pK_{app.}$ for the isomerisation of ferricytochrome *c* is 9 ([47] and own measurements on 695 nm band). For the cytochrome *c* wavelength triplet the contributions by the 'low pH' and 'high pH' difference spectra were found to be 0.70 and 0.58 $mM^{-1} \cdot cm^{-1}$, respectively, and for the haem *a* wavelength triplet, −0.26 and −0.18 $mM^{-1} \cdot cm^{-1}$, respectively.

(2) The method of simulation

Fig. 7 is a representation of the model system discussed in the main text. The arrows point in the direction of electronation or deprotonation as shown. Ratios, $R_{e,x}$ for electronation, and $R_{h,x}$ for deprotonation, can be defined as:

$$R_{e,x} = [\text{red.}]/[\text{ox.}] = 10^{((E_{m,x} - E_h)/58)} \quad (\text{at } 20\,^\circ\text{C}) \quad (5)$$

$$R_{h,x} = [\text{deprot.}]/[\text{prot.}] = 10^{(\text{pH} - pK_x)} \quad (6)$$

The solid arrows 'connect in' all of the possible substates of the system. The number of solid arrows is the number of equilibria needed to define the whole system, the choice of equilibria being arbitrary provided that there is only one route between any two substates, i.e., the solid arrows from a 'tree' and not a network.

The general method of simulation is as follows. We start with an arbitrary 'root' substate for which the concentration is set at unity. The concentrations of the

remaining substates are then easily obtained using the ratios (calculated for the chosen values of E_h and pH, as appropriate), and the occupancy of a particular substate (or set of substates) is given by the concentration of that substate (or the sum of the concentrations of the substates in the set) divided by the sum of the concentrations of all the substates. For example, using the model shown in Fig. 7, if we choose substate '00^H' as the root substate then the concentrations of substates '00^H', '10^H', '00', '10' and '11' are 1, $R_{e,[]0^H}$ $R_{h,00}$, $R_{h,00} \cdot R_{e,[]0}$ and $R_{h,00} \cdot R_{e,[]0} \cdot R_{e,1[]}$, respectively. The occupancy of the set of substates in which component 1 is reduced, i.e., '10^H', '11^H', '10' and '11' is given by Eqn. 7:

fractional reduction of component 1

$$= \{ R_{e,[]0^H} + R_{e,[]0^H} \cdot R_{e,1[]^H} + R_{h,00} \cdot R_{e,[]0} + R_{h,00} \cdot R_{e,[]0} \cdot R_{e,1[]} \} \times \{ 1 + R_{e,[]0^H} + R_{e,0[]^H} + R_{e,[]0^H} \cdot R_{e,1[]^H} + R_{h,00} + R_{h,00} \cdot R_{e,[]0} + R_{h,00} \cdot R_{e,0[]} + R_{h,00} \cdot R_{e,[]0} \cdot R_{e,1[]} \}^{-1} \quad (7)$$

At a given pH the two-state system shown in Fig. 7 is analogous to a single-state system, i.e., it can be described using three apparent midpoint potentials, the apparent interaction (I') between the components, if any, being given by the difference for either component between its apparent midpoint when the other component is oxidised and its apparent midpoint when the other component is reduced. These apparent midpoints can be obtained using Eqn. 5. For example $E_{m,[]0^0}$ for component 1, is obtained as follows:

$$R_{e,[]0^0} = \frac{R_{e,[]0^H} + R_{h,00} \cdot R_{e,[]0}}{1 + R_{h,00}} = 10^{((E_{m,[]0^0} - E_h)/58)} \quad (\text{at } 20\,^\circ\text{C}) \quad (8)$$

Hence:

$$E_{m,[]0^0} = 58 \cdot \{ \log_{10}(R_{e,[]0^H} + R_{h,00} \cdot R_{e,[]0}) - \log_{10}(1 + R_{h,00}) \} + E_h \quad (9)$$

Acknowledgements

This work was supported by the SERC (grant GR/F/17605). We are also indebted to other benefactors, named in the brochure of the U.K. Registered Charity named the Glynn Research Foundation Ltd., for general financial support of the research facilities at the Glynn Research Institute. We are grateful to Robert Harper for preparation of the cytochrome-*c* oxidase and for help in preparing the manuscript, and to Alan Jeal for assembly of the spectrophotometer and flash unit. We thank Roy Mitchell, Ian West and Peter Mitchell for useful discussions, and Mårten Wikström for his comments on the manuscript.

References

1 Wikström, M., Krab, K. and Saraste, M. (1981) Cytochrome Oxidase. A Synthesis, pp. 1–198, Academic Press, London.
2 Steffens, G.C.M. and Buse, G. (1988) EBEC Rep. 5, 100.
3 Nicholls, P. and Petersen, L.C. (1974) Biochim. Biophys. Acta 357, 462–467.
4 Wikström, M.K.F., Harmon, H.J., Ingledew, W.J. and Chance, B. (1976) FEBS Lett. 65, 259–277.
5 Wilson, D.F., Lindsay, J.G. and Brocklehurst, E.S. (1972) Biochim. Biophys. Acta 256, 277–286.
6 Tiesjema, R.H., Muijsers, A.O. and Van Gelder, B.F. (1973) Biochim. Biophys. Acta 305, 19–28.
7 Minnaert, K. (1965) Biochim. Biophys. Acta 110, 42–56.
8 Gorren, A.C.F., Dekker, H. and Wever, R. (1985) Biochim. Biophys. Acta 809, 90–96.
9 Artzatbanov, V.Yu., Konstantinov, A.A. and Skulachev, V.P. (1978) FEBS Lett. 87, 180–185.
10 Wilson, D.F. and Leigh, J.S. (1974) Ann. N.Y. Acad. Sci. 227, 630–635.
11 Kojima, N. and Palmer, G. (1983) J. Biol. Chem. 258, 14908–14913.
12 Goodman, G. (1984) J. Biol. Chem. 259, 15094–15099.
13 Blair, D.F., Ellis, W.R., Wang, H., Gray, H.B. and Chan, S.I. (1986) J. Biol. Chem. 261, 11524–11537.
14 Nicholls, P. and Wrigglesworth, J.M. (1988) Ann. N.Y. Acad. Sci. 550, 59–67.
15 Wikström, M. (1989) Ann. N.Y. Acad. Sci. 550, 199–206.
16 Ellis, W.R., Wang, H., Blair, D.F., Gray, H.B. and Chan, S.I. (1986) Biochemistry 25, 161–167.
17 Wang, H., Blair, D.F., Ellis, W.R., Gray, H.B. and Chan, S.I. (1986) Biochemistry 25, 167–171.
18 Rich, P.R. (1988) Ann. N.Y. Acad. Sci. 550, 254–259.
19 Rich, P.R., West, I.C. and Mitchell, P. (1988) FEBS Lett. 233, 25–30.
20 Ahmad, I., Cusanovich, M.A. and Tollin, G. (1982) Biochemistry 21, 3122–3128.
21 Ahmad, I., Cusanovich, M.A. and Tollin, G. (1981) Proc. Natl. Acad. Sci. USA 78, 6724–6728.
22 Moody, A.J. and Rich, P.R. (1988) EBEC Rep. 5, 69.
23 Erecinska, M., Chance, B. and Wilson, D.F. (1971) FEBS Lett. 16, 284–286.
24 Wilson, D.F., Erecinska, M. and Owen, C.S. (1976) Arch. Biochem. Biophys. 175, 160–172.
25 Moody, A.J., Mitchell, R. and Rich, P.R. (1989) Biochem. Soc. Trans. 17, 895–896.
26 Moody, A.J. and Rich, P.R. (1989) Biochem. Soc. Trans. 17, 896–897.
27 King, T.E. (1961) J. Biol. Chem. 236, 2342–2346.
28 Kuboyama, M., Yong, F.K. and King, T.E. (1972) J. Biol. Chem. 247, 6375–6383.
29 Prince, R.C., Linkletter, S.J.G. and Dutton, P.L. (1981) Biochim. Biophys. Acta 635, 132–148.
30 Vanneste, W.H. (1988) Biochemistry 5, 838–848.
31 Margoliash, E. and Frohwirt, N. (1959) Biochem. J. 71, 570–572.
32 George, P. and Tsou, C.L. (1952) Biochem. J. 50, 440–448.
33 Michaelis, L., Schubert, M.P. and Granick, S. (1939) J. Am. Chem. Soc. 61, 1981–1992.
34 Blair, D.F., Bocian, D.F., Babcock, G.T. and Chan, S.I. (1982) Biochemistry 21, 6928–6935.
35 Baker, G.M., Noguchi, M. and Palmer, G. (1987) J. Biol. Chem. 262, 595–604.
36 Brandt, U., Schägger, H. and Von Jagow, G. (1988) EBEC Rep. 5, 89; (1989) Eur. J. Biochem. 182, 705–711.
37 Nicholls, P. and Chanady, G.A. (1982) Biochem. J. 203, 541–549.
38 Dervartanian, D.V., Lee, I.Y., Slater, E.C. and Van Gelder, B.F. (1974) Biochim. Biophys. Acta 347, 321–327.

39 Johnson, M.K., Eglinton, D.G., Gooding, P.E., Greenwood, C. and Thomson, A.J. (1981) Biochem. J. 193, 699–708.
40 Tsudzuki, T. and Wilson, D.F. (1971) Arch. Biochem. Biophys. 145, 149–154.
41 Lindsay, J.G., Owen, C.S. and Wilson, D.F. (1975) Arch. Biochem. Biophys. 169, 492–505.
42 Wikström, M. (1982) Electron transport and oxygen utilisation (Chien Ho, ed.), pp. 271–277, Macmillan, London.
43 Krab, K. and Wikström, M. (1987) Biochim. Biophys. Acta 895, 25–39.
44 Mitchell, R. and Mitchell, P. (1989) Biochem. Soc. Trans. 17, 892–893.
45 Wikström, M. (1989) Nature 338, 776–778.
46 Rich, P.R., Moody, A.J. and Mitchell, R. (1989) in Charge and Field Effects in Biosystems (Allen, M.J., ed.), pp. 7–20, Plenum, New York.
47 Davis, L.A., Schejter, A. and Hess, G.P. (1974) J. Biol. Chem. 249, 2624–2632.
48 Jones, M.G., Bickar, D., Wilson, M.T., Brunori, M., Colosimo, A. and Sarti, P. (1984) Biochem. J. 220, 57–66.